Dynamic PEM Fuel Cell Model for Power Electronics Design with Temperature Consideration

Ken Stanton, *Member, IEEE,* Jih-Sheng (Jason) Lai, *Fellow, IEEE*, and Douglas Nelson

***Abstract*—A dynamic model of a PEM fuel cell is developed for power electronics simulation. The model accounts for static losses of activation, ohmic, and concentration regions, and dynamic transients due to charge double layer and compressor delay. In this paper, study was given to additional factors, including temperature, for their effects on the output voltage with respect to load on the fuel cell stack. Findings were analyzed and incorporated into the model based on testing with a Ballard Nexa 1.2 kW PEM fuel cell unit. The model is developed for PSPICE, then tested and compared to experimental data from the Ballard fuel cell system.**

***Index Terms*—Proton Exchange Membrane (PEM), fuel cell, modeling, power electronics, dynamics.**

I. Introduction

FUEL cell systems are finding use in various power applications, including automotive, residential, and commercial. They show great promise, as they can utilize hydrogen as fuel and produce water and heat as byproducts, with relatively few moving parts and high efficiency compared to combustion devices. The proton exchange membrane fuel cell (PEMFC) has a low working temperature, is compact and has good power density, and can respond quickly to power demand changes, relative to other types of fuel cells.

In most applications, power electronics are required in order to use the PEMFC as the power source. The fuel cell is considered a voltage source, with its output level depending on power demanded of it. As such, applications that require a constant or otherwise controlled voltage level must have power conditioning electronics such as dc/dc converters.

Designing power electronics for fuel cell applications has some challenges, including transient power handling and system control with large variations in output voltage over the operating range. Whether or not such issues can be effectively designed for depends highly on the quality of the fuel cell model used in simulation. Software packages such as PSPICE, MATLAB, SIMULINK, and SABER accept the power electronics and loads readily, so a fuel cell model is needed that can be used with these programs as well. Fig. 1 shows an example fuel cell system to be simulated, including the fuel cell, power electronics, and load.

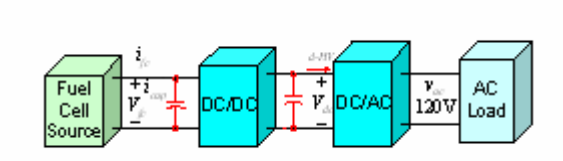

Fig. 1: Power electronics system driving ac load, powered by a fuel cell.

A great number of fuel cell models exist, and for many different types of simulation software. Extensive models can be found in [1]-[6], all of which have fuel cell equations directly entered into the model. Of these, [1], [2], and [4] develop models in PSPICE, [2] and [6] in MATLAB/ SIMULINK, and [1] also in MathCAD; models in [3] and [5] are not applied to any specific software packages. References [7] and [8] develop fuel cell models using electrical components and simple behavior blocks in PSPICE. Finally, [9] and [10] explain fuel cell equations in great detail, discuss modeling results, but don't specifically show the models. All papers above are for PEMFC's except for [6], which is for a solid-oxide fuel cell (SOFC).

The extensive models [1]-[6] provide very accurate output voltage and currents, as well as providing outputs like temperature and air humidity. However, these models are slow to simulate, cumbersome to use, and require extensive knowledge of inputs to the fuel cell. Electrical models in [7] and [8] resolve these problems, but lose accuracy in the output as the temperature and hydration of the fuel cell system are not considered.

The work presented in this paper takes the model shown in [8] and adds large time-constant dynamics, primarily due to temperature. Temperature effects cannot be isolated, so other factors including hydration, humidity, cooling system, and the

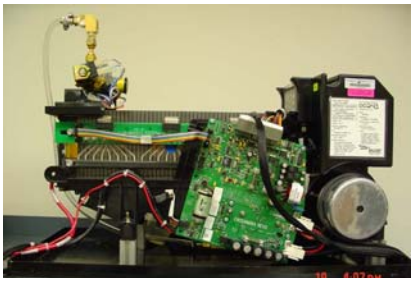

Fig. 2: Ballard NEXA 1.2kW PEM fuel cell system, including hydrogen pressure regulator, air compressor, and control system with sensors. This system was used for the development work in this paper.

Manuscript received xxx. This work is sponsored by the U.S. Department of Energy (DOE) National Energy Technology Laboratory (NETL) Solid-State Energy Alliance Program (SECA) under Award Number DE-FC26-02NT41567. The Ballard Nexa 1.2kW PEMFC was provided by American Power Converison Corp., whose donation allowed this research to happen.

Ken Stanton is a Ph.D. student with the Electrical and Computer Engineering Department, Virginia Tech, Blacksburg, VA, 24060, USA (e-mail: kstanton@vt.edu).

Jih-Sheng (Jason) Lai is a professor with the Electrical and Computer Engineering Department, Virginia Tech, Blacksburg, VA, 24060, USA (e-mail: laijs@vt.edu).

control system are inherently present. At a given load condition, a rise in output voltage can be observed over a time period of minutes, the net effect of which is addressed herein. Additionally, the causes of these dynamics are studied in detail, with a focus on the role of temperature. Development testing was performed with a Ballard Nexa 1.2 kW PEMFC system, shown in Fig. 2.

II. Basic PEMFC Operation and Equations

This section presents basic background information on fuel cell operation, supported by equations. For this work, some assumptions were made to simplify both equations and analysis, as follows [2]:

1. All gases behave ideally and are distributed uniformly.
2. The fuel is humidified H_2 and the oxidant is humidified ambient air.
3. Thermodynamic properties are evaluated at the average stack temperature, temperature variations across the stack are neglected, and the overall specific heat capacity of the stack is constant.
4. Parameters of individual cell performance can be lumped together to represent a fuel cell stack.

A. Static Operational Conditions of PEMFC

For any given load condition in the operational range of a PEMFC, certain factors govern the output; Fig. 3 shows this graphically in the typical I-V fuel cell curve. These factors are shown below, observed for a single fuel cell in a fuel cell stack. The output voltage of a given fuel cell is

$$V_{cell} = E_{cell} - V_{act,cell} - V_{ohm,cell} - V_{conc,cell}, \quad (1)$$

and therefore the stack output voltage is

$$V_{out} = V_{cell} \times N_{cell} = E - V_{act} - V_{ohm} - V_{conc}, \quad (2)$$

where N_{cell} is the number of cells in the stack [2]. All other nomenclature in (1) is defined below.

1) Open Circuit Voltage: A fuel cell can be considered a voltage source, having an ideal voltage level which is reduced by properties of its operation. In the PEMFC, there is the ideal voltage output, E, which is often called the open circuit voltage[1] (OCV), or theoretical reversible voltage. This voltage is calculated as

$$E_{cell} = E_{0,cell} + \frac{RT}{2F}\ln\left[p^*_{H_2} \times \sqrt{p^*_{O_2}} \right] - E_{d,cell}, \quad (3)$$

where R is a gas constant, T is temperature in Kelvin, F is Faraday's constant, and p^* is the partial pressure of the noted species, all of which are positive. Furthermore,

$$E_{0,cell} = E^0_{0,cell} - k_E(T - 298), \quad (4)$$

where $E^0_{0,cell}$ is the reference potential at standard temperature and pressure (298 K, 1 atm), and k_E is a constant, both positive.

$$E_{d,cell}(t) = \lambda_e i(t)[1 - \exp\left(-\frac{t}{\tau_e}\right)] \quad (5)$$

is the final element of the OCV equation, where λ_e is a constant, $i(t)$ is the cell current, and τ_e is fuel and oxidant flow delay, all positive.

2) Activation Polarization: Under low power demands, the electrochemical reaction is slow at the electrode surface due to the nature of its kinetics [7]. This loss of potential is

$$V_{act} = \eta_0 + a(T - 298) + bT\ln(I), \quad (6)$$

where a, b, and η_0 are constants, all positive [2]. Activation polarization therefore has a natural log curve over the range of current loads, as can be seen in Fig. 3.

3) Ohmic Polarization: This region is largely linear, as it relates to loss of potential due to electrical resistance of the polymer membrane, between the membrane and electrodes, and in the electrodes themselves. The ohmic losses can be expressed as

$$V_{ohm} = IR_{ohm} \quad (7)$$

with

$$R_{ohm} = R_{ohm0} + k_{RI}I - k_{RT}T, \quad (8)$$

which has respective k constants for both the current and temperature dependent terms, and a constant term R_{ohm0}, all positive.

4) Concentration Polarization: This loss, also called mass-

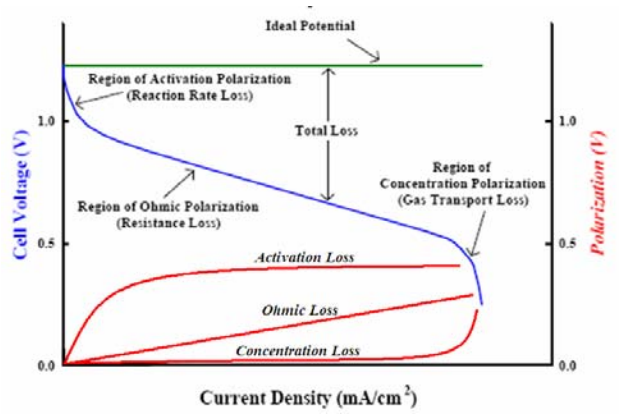

Fig. 3. Typical fuel cell polarization, or I-V, curve. Ideal potential (top) is reduced by three polarization regions (bottom three curves), to the commonly seen result (second from top).

[1] The terminology "open circuit voltage" is commonly used in fuel cell literature, but can be confusing to those in electronics. Here it is meant as the voltage level if no polarization losses were present.

transportation loss, occurs at high current loads due to an inability to supply reactants and remove products fast enough for the chemical reaction to occur completely. The concentration polarization is defined as

$$V_{conc} = -\frac{RT}{zF}\ln\left(1-\frac{I}{I_{\lim}}\right) \quad (9)$$

where z is the number of electrons participating, and I_{lim} is the limitation current, both positive. The curve can be observed in Fig. 3 by the severe drop-off at high current demand. It should be noted that fuel cells are typically designed to avoid operating in this region.

B. *Dynamic Operating Conditions of PEMFC*

Major short time-constant dynamic conditions can be observed during load transients in Fig. 4. When a load step occurs, the short-term fuel cell response is dominated by two major phenomena: mass transport loss and compressor speed delay. Mass transport delay occurs when there is a deficiency (or excess) of reactants (products) at the reaction site. The fuel cell voltage drops (rises) like a capacitor due to the charge double layer effect. This effect is capacitor-like because of the physical structure of the fuel cell electrodes separated by the membrane. The voltage drop (spike) occurs due to a delay in change of the compressor speed, which supplies ambient air, and needs to adjust to the load demand. In Fig. 4, the dip in fuel cell voltage shows both of these phenomena, with the initial falling curve a result of mass transport loss's capacitance, and the recovery occurring as the compressor comes to speed. These are both first order responses, so for a time simulation, they can be modeled with

$$V_{cdl} = e^{-t/\tau_2} - 1 \quad (10)$$

and

$$V_{comp} = 1 - e^{-t/\tau_1}, \quad (11)$$

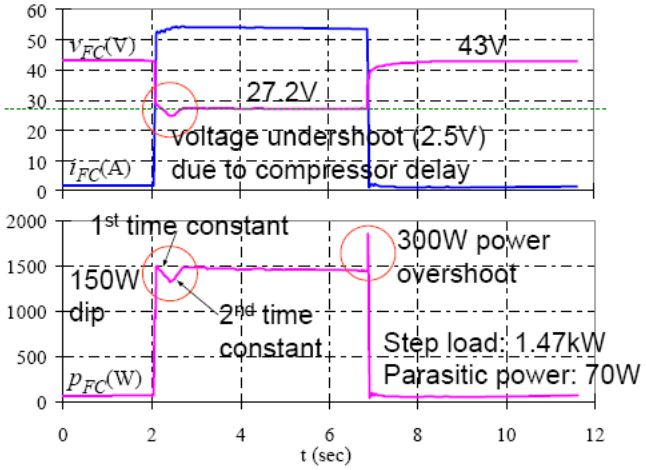

Fig. 4. Short time-period fuel cell dynamic showing no- to full-load step. Transient points of interest are circled on voltage and power curves.

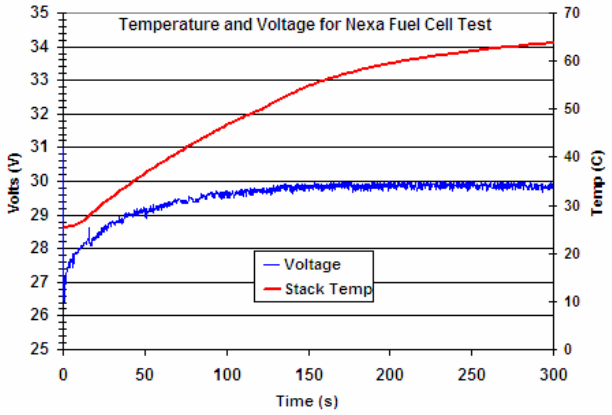

Fig. 5. Temperature (upper curve) and voltage (lower curve) data for a full-load step transient, showing long time-constant rises in both. This gave motivation to improve fuel cell models that do not incorporate these long time transients.

where τ_1 and τ_2 are respective time constants for the charge double layer discharge and compressor speed change. The charge double layer time constant is on the order of a few microseconds, and the compressor time constant around a hundred milliseconds. The resulting dynamic transient is the sum of (10) and (11).

The dynamic conditions are important for an accurate model, as power electronics designers need to consider energy storage if they wish to suppress these effects.

C. *Additional Dynamics of PEMFC, Including Temperature*

In Fig. 5, a load step occurred, increasing from no-load to full-load at time t=0. (Note: the dynamics discussed in section B cannot be seen in this figure.) There is a voltage dynamic present, on the order of many seconds, which was not included in the previous sections. This transient is the focus of the model improvements made in this paper.

At first, it appeared that this transient was solely influenced by stack temperature. According to [2],

$$\dot{q}_{net} = \dot{q}_{chem} - \dot{q}_{elec} - \dot{q}_{sens+latent} - \dot{q}_{loss}, \quad (12)$$

where q refers to energy and $\dot{q}$ is power. Therefore net power is the power released by the chemical reaction reduced by electrical power, heat power due to reactants and products flowing through the stack (sensible and latent), and power lost to the surroundings (by heat). This net power is that responsible for changes in fuel cell temperature, as given by

$$M_{FC}C_{FC}\frac{dT}{dt} = \dot{q}_{net}, \quad (13)$$

where M_{FC} is the total mass of the fuel cell and C_{FC} is its specific heat capacity. Equations (12) and (13) could be used to predict stack temperature if the terms of (12) could be evaluated well and evaluated simply. However, the equations behind those terms, as given in [2], require extensive

knowledge of fuel and air characteristics to be known, and also depend on temperature themselves. As well, data from tests with the Ballard fuel cell system support this notion, i.e. a solid relationship between electrical characteristics and stack temperature was simply not attainable. Therefore, if the model being developed is to remain simple and reliable, temperature prediction directly should not be attempted.

Despite this, it is still apparent that the voltage transient is related to temperature. Fig. 4.2 in [1] shows increasing stack temperature as generally causing an increase in output voltage, i.e. it shifts the I-V curve upward. As well, [2], [3], [5], and [9] state that the power consumed by static polarization losses is considered the heat source for fuel cell temperature change, and this power increases with stack output power demanded. Therefore, in load step dynamics like that of Fig. 5, it can be concluded that there is a direct relationship between changing stack temperature, changing output power, and changing output voltage.

Based largely on this, it was noted that as power demanded of the fuel cell stack changed, so did the polarization losses. These losses are the major contributors to stack heating and cooling, so therefore power demanded of the stack is related to stack temperature. As temperature changes, along with other factors such as cell hydration, so does the magnitude of the polarization losses, even at a constant load condition. As these losses change, the output voltage of the stack is directly affected. Therefore, it was concluded that there should be a correlation between the power demanded of the fuel cell stack and the stack's output voltage, via changes related to temperature. This hypothesis is the basis of the model proposed herein, and was tested and developed. Section III will display and discuss the results.

D. Other Operation Modes for Fuel Cell System

Over and above standard operation, the tested Ballard Nexa fuel cell system has additional operating modes, including a protective shutdown. These modes should be considered if creating an extensive fuel cell system model.

1) Cold Start Operation: When started from a cold condition (stack temperature less than or equal to ambient), Ballard's control system operates in cold start mode. This is a protective mode that limits output power, approximately 300-500 W, for 2 minutes. If the load attempts to exceed the power level in the set time, the fuel system goes into shutdown mode, suspending all activity.

2) Protective Shutdown: Protective shutdown of the fuel cell system occurs whenever a measured parameter exceeds its preset limit. These parameters include fuel pressure, stack temperature, power output, and fuel (hydrogen) leakage. In such an event, all output is stopped and fuel cell operation ceased.

3) Rejuvenation Mode: Part of normal shutdown, the fuel cell system disconnects itself from the output and runs independently to control hydration of the stack. This mode would not need to be modeled (unless including fuel consumption), as it is part of normal shutdown and does not produce any electrical output [11].

III. Power Based Model Development

A. Data Collection and Analysis

Dozens of load step curves were captured and analyzed from the Ballard Nexa fuel cell system via its serial PC connection. The data were collected and analyzed in Fig. 6. Change in voltage was calculated by subtracting the post-transient voltage level from the results of a fast load sweep, which would keep temperature relatively constant. A linear curve-fit was then used to estimate the results, with only a few major outliers. These outliers and other differences in values from test to test can be attributed to:

1. Ambient variations including temperature, humidity, air quality, and fuel cell containment
2. Fuel variations including purity and humidity
3. Hydration level of the stack
4. Age degradation of stack, or damage to it
5. Variations in sensors, compressor integrity, or other physical variations of balance of plant components
6. Variations in the integrity of the load under test

The result presented here can be interpreted as such: if a load step were performed from a steady-state no-load condition, then the voltage can be expected to change by the amount specified, after the large time-constant transient is complete. For the Ballard Nexa system tested, the linear curve-fit has a slope of 2.2 V/kW. Therefore, for a 1.2 kW (full-load) step, the voltage will change 2.5 V from start to finish of the transient. Since output voltage at this point is 28.5 V, this amounts to nearly a 10% change in voltage – a very significant level to a power electronics designer.

B. Load Dependent Model

The fuel cell model in [8] includes all the static and dynamic conditions discussed in section II A & B. The model proposed here extended this work by adding the relationship from the discussion in section III A.

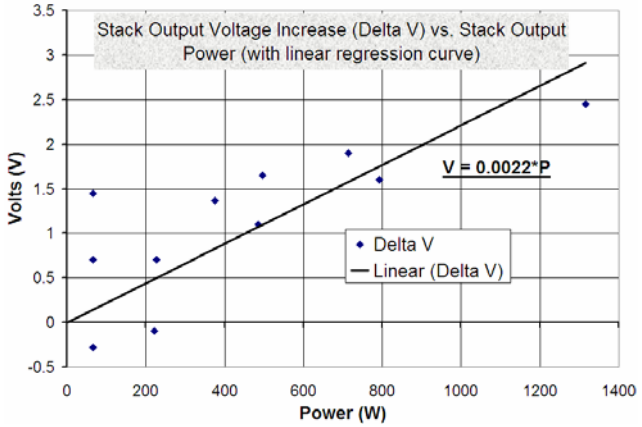

Fig. 6. Stack output voltage change for a given load condition. This general relationship is the basis for the power based model.

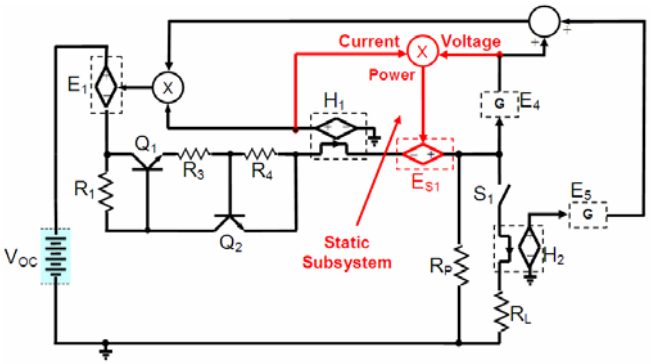

Fig. 7. Fuel cell model with static modification subsystem added.

1) Static Modification: The static subsystem of the model is established by calculating stack output power, as product of current and voltage, and feeding this into a voltage-dependent voltage-source (VDVS). The VDVS has a gain of 2.2 V/kW as calculated, and is oriented such that positive stack power creates an increase in the model's output voltage. A simplified block diagram of this system can be seen in Fig. 7. Note that this diagram has no dynamic components.

When the static subsystem is implemented, a shift in the static I-V curve occurs. Fig. 8 illustrates this. The lower, darker curve was created by taking data directly from [11]. Following, the upper, lighter curve was created by adding the linear 2.2 V/kW increase to the other curve, illustrating the difference in steady-state output voltage.

2) Dynamic Modification: During a load-step transient, output voltage changes exponentially over time. As stated previously, this is primarily due to temperature changes, but hydration, humidity, etc. can also affect this curve. The dynamic being modeled has an exponential response over time, so a LaPlace block is used to simulate it (block E_{S2}). The LaPlace block takes in the output of the static block and applies it to

$$G_{LaPlace}(s) = \frac{1}{\tau s + 1}, \tag{16}$$

where τ is the dynamic time constant, thereby creating an exponential response to the transient. A block diagram of the model with the dynamic subsystem can be seen in Fig. 9.

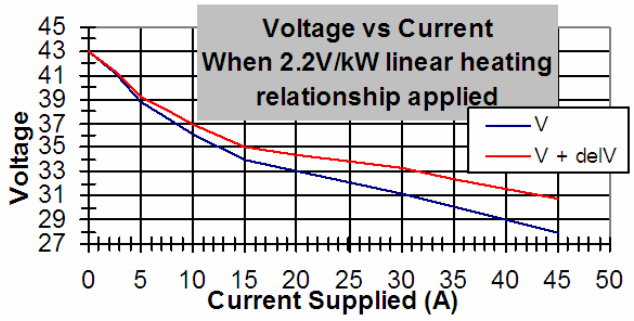

Fig. 8. I-V curve of Ballard Nexa fuel cell. Lower curve is original output voltage curve, taken from [11]. Upper curve is output voltage with the static subsystem in effect.

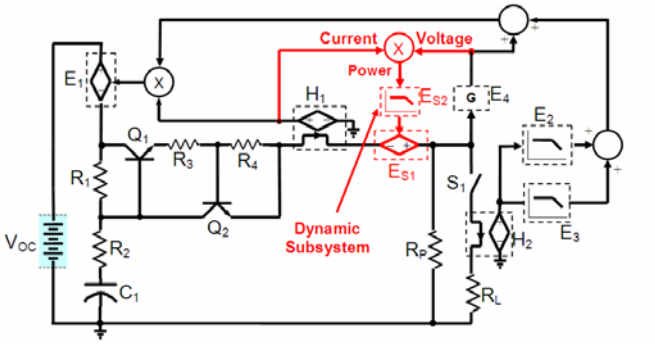

Fig. 9. Fuel cell model with dynamic subsystem modification added.

C. Setting Model Parameters for Ballard System

To use the proposed model for the Ballard Nexa fuel cell system, only a single time constant needs to be determined. The time constant must be chosen carefully, as it is highly related to temperature, which can be altered by the Ballard controls via the cooling fan and compressor. As a result, small load step simulations will be highly accurate, as the temperature controls are unlikely to change. Alternately, it can be argued that large load steps include all of these effects, and therefore are more representative of the system holistically.

Testing on the Ballard system led to a fairly consistent dynamic time constant of 50 seconds, for both large and small load steps. This value is entered into (16) to complete the model modification for the Ballard fuel cell system.

D. Fuel Cell Model Operation

The model demonstrated in this paper has many components and component systems representing fuel cell phenomena. These phenomena have been discussed in section II, including static polarizations and dynamics such as charge double layer. A description of how the fuel cell characteristics are modeled with electrical components in Figs. 8 and 9 follows. Additionally, values of these components are all shown in Table 1.

Considering first the static operation of Fig. 8, the circuit has two current flow paths. When the load current is low, the

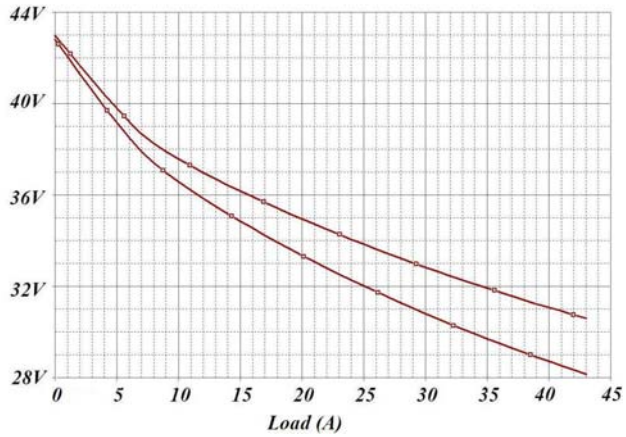

Fig. 10. I-V curve from simulation of PSPICE model set up for Ballard fuel cell system. Upper curve represents electrical model with proposed modification in effect, and lower curve without. The lower curve closely matches that found in [11] for the Ballard system.

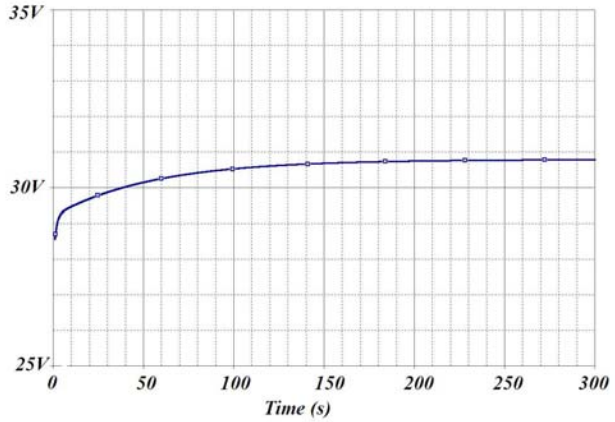

Fig. 11. Full-load step simulation using PSPICE model developed.

power flows through Q_1, R_3, and R_4 to the load. With R_4 voltage drop being low, transistor Q_2 will be cut off. This operating condition represents the activation polarization region. As the load current increases, the R_4 voltage eventually exceeds the required base-emitter junction voltage, and Q_2 starts conducting. At this time, operation is in the middle region of the I-V curve of Fig. 3, dominated by ohmic losses. In this model, the combination of resistances R_1, R_3, R_4, and collector-emitter junction impedances model the actual ohmic loss. Concentration polarization is not modeled directly as the Ballard system (as well as most others) are designed such that they never operate statically in this region.

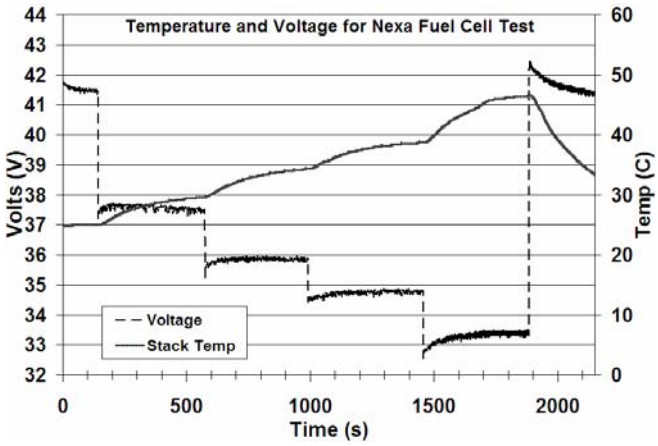

Fig. 12. Experimental test results for 4 load steps performed on Ballard fuel cell system.

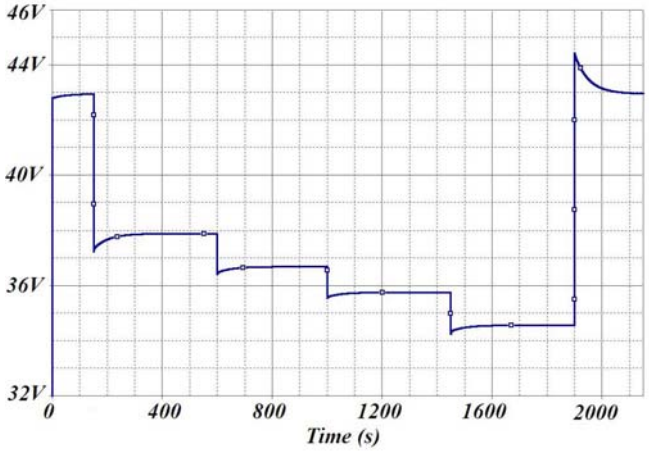

Fig. 13. Simulation results from PSPICE model developed for he same load conditions in Fig. 12.

The dynamic model of Fig. 9 employs two first-order dynamic blocks, E_2 and E_3, to represent the load transient effect. The first time constant (E_3) is the charge double-layer effect, which is in the order of sub-microsecond, and the second time constant (E_2) is the compressor delay, which is in the order of sub-second. As a transient load applies, with a nearly invisible 1st time constant delay, a load current-controlled voltage source (CCVS) quickly increases the multiplier output to increase E_1 drop, and thus the output voltage drops. When the output voltage decreases, the multiplier input also decreases with a delay related to the 2nd time constant, the compressor delay. Consequently, the multiplier output and the E_1 drop decreases, thus bringing the output back higher, which represents the effect of the air compressor.

IV. Model Validation

After completing the modified fuel cell model in PSPICE, simulations were run to compare to experimental fuel cell test results. The simulations were set up to match the timing and magnitude of loads applied in the experimental tests.

1) I-V Curve: The first simulation is a load sweep from zero to full-load current, with and without the model modification active. The result is shown in Fig. 10, with the lower curve representing the output without the proposed dynamic modification, and upper with modification. This result closely matches that of Fig. 8, the static modeling goal.

2) Dynamics: Fig. 11 shows the result of a full-load step transient simulation, and can be compared to Fig. 5. At time t=0, a load step occurred, increasing from no-load to full-load. First, note that the voltage level of the simulation is higher than the experimental result. This is largely attributed to age of the Ballard fuel cell system, which has degraded in its ability to output its full potential; other such factors were listed in section III A.

Additionally, a simulation was run to compare to a series of part-load steps performed on the Ballard system. The experimental test started at no-load, stepped to 225 W, 360 W, 480 W, and 680 W for 450 s each, and then back to no-load; the simulation followed the same pattern. Fig. 12 shows the experimental result, and Fig. 13 shows the simulation. Again, note that a slightly higher voltage level is observed in the simulation, as mentioned previously. Also, a small drop in voltage appears during the first load step in Fig. 12. It is possible that this load condition was near the border of two compressor or cooling fan speeds, and the speed changed during this load condition test. This phenomenon was not accounted for in the model developed, and hence will not appear in Fig. 13.

V. Conclusion

Previous fuel cell models are either over-complicated or over-simplified, making them poorly suited for many

applications. In this paper, an expanded electrical model of a PEMFC was proposed and tested, and results compared to experimental data. The results show that the proposed model is more representative of actual fuel cell output than previous simple electrical models discussed in the introduction. To achieve this, the previous model was improved by adding a temperature-related dynamic observed over a period of many seconds. Also, the model is simpler to set up and use than the more complicated models available previously. It can be used as-is to simulate a Ballard Nexa 1.2 kW system, or its values can be modified for another PEMFC using minimal test data. Since the goal of this work was to improve electrical modeling state-of-the-art while maintaining model simplicity and fast simulation speed, the work was a success. The power electronics designer can use this model to simulate an entire system, such as that suggested in Fig. 1, and experience improved representation of fuel cell output characteristics over some previous models.

APPENDIX

TABLE I
MODEL COMPONENT VALUES

Symbol	Value / Equation	Units	Description
R_1	0.036	Ω	High current branch resistor
R_2	0.01	Ω	Model internal filter resistor
R_3	0.32	Ω	High current branch control resistor 1
R_4	0.061	Ω	High current branch control resistor 2
R_P	25.0	Ω	Parasitic Load Resistor
R_L	0.65–inf	Ω	Load
C_1	2.0	uF	Model internal filter capacitor
E_1	1	(gain)	Transient voltage-drop block
E_2	-0.75/ (1+1.2s)	(gain)	Compressor delay modeling block
E_3	0.05/ (1+0.12s)	(gain)	Charge double layer modeling block
E_4	0.06	(gain)	Output voltage scaling
E_5	-0.004	(gain)	Output current scaling
E_{S1}	0.27	(gain)	Subsystem VCVS
E_{S2}	1/(1+50s)	(gain)	Subsystem dynamic LaPlace block
H_1	0.16	(gain)	Fuel cell current CCVS
H_2	0.16	(gain)	Load current CCVS
Q_1	100	Area	QbreakN setting
Q_2	10e6	Area	QbreakN setting
V_{OC}	45	V	Ideal (open-circuit) fuel cell voltage

REFERENCES

[1] Jerome Ho Chun Lee, "A Proton Exchange Membrane Fuel Cell (PEMFC) Model for Use in Power Electronics," M.S. thesis, Dept. of Electronic and Information Eng., The Hong Kong Polytechnic Univ., Hung Hom, Hong Kong, 2004.

[2] C. Wang, M. H. Nehrir, and S. R. Shaw, "Dynamic Models and Model Validation for PEM Fuel Cells Using Electrical Circuits," *IEEE Trans. Energy Conv.*, vol. 20, no. 2, pp. 442-451, June 2005.

[3] P. Srinivasan, J. E. Sneckenberger, and A. Feliachi, "Dynamic Heat Transfer Model Analysis of the Power Generation Characteristics for a Proton Exchange Membrane Fuel Cell Stack," in *Proc. 35th Southeastern Symp. on Sys. Theory,* Mar. 2003, pp. 252-258.

[4] P. Famouri and R. S. Gemmen, "Electrochemical Circuit Model of a PEM Fuel Cell," at *Power Eng. Soc. Gen. Meeting*, July 2003, pp. 1440-1444.

[5] X. Kong, A. M. Khambadkone, and S. K. Thum, "A Hybrid Model With Combined Steady-state and Dynamic Characteristics of PEMFC Fuel Cell Stack," in *Conf. Record 2005 Ind. App. Conf.,* Oct. 2005, pp. 1618-1625.

[6] K. Sedghisigarchi and A. Feliachi, "Dynamic and Transient Analysis of Power Distribution Systems With Fuel Cells-Part I: Fuel-Cell Dynamic Model," *IEEE Trans. Energy Conv.,* Vol. 19, no. 2, pp. 423-428, June 2004.

[7] D. Yu and S. Yuvarajan, "A Novel Circuit Model For PEM Fuel Cells," at *Applied Power Elect. Conf. and Exp.,* 2004, pp. 362-366.

[8] Jih-Sheng Lai, "A Low-Cost DC/DC Converter for SOFC," presented at SECA Annual Review Meeting, Boston, MA, May 2004.

[9] W. Friede, S. Raël, and B. Davat, "Mathematical Model and Characterization of the Transient Behavior of a PEM Fuel Cell," *IEEE Trans. Power Elects.,* Vol. 19, no. 2, pp. 1234-1241, Sep. 2004.

[10] J. M. Corrêa, F. A. Farret, L. N. Canha, and M. G. Simões, "An Electrochemical-Based Fuel-Cell Model Suitable for Electrical Engineering Automation Approach," *IEEE Trans. Ind. Elects.,* Vol. 51, no. 5, Oct. 2004.

[11] *Nexa Power Module User's Manual,* Ballard Power Systems Inc., Document Number MAN5100078, June 2003.